An Accurate Calculation of Electronic Contribution to Static Permittivity Tensor for Organic Molecular Crystals on the Basis of the Charge Response Kernel Theory

Jun'ya Tsutsumi,*,†,‡ Hiroyuki Yoshida,† Richard Murdey,§ Shigeki Kato,‖ and Naoki Sato*,†

Institute for Chemical Research, Kyoto University, Uji, Kyoto 611-0011, Japan, Pioneering Research Unit for Next Generation, Kyoto University, Uji, Kyoto 611-0011, Japan, and Department of Chemistry, Graduate School of Science, Kyoto University, Sakyo-ku, Kyoto 606-8502, Japan

Received: April 14, 2009; Revised Manuscript Received: June 22, 2009

We have developed a new method to calculate the static permittivity tensors of organic molecular crystals by applying the charge response kernel theory (Morita, A.; Kato, S. *J. Am. Chem. Soc.* **1997**, *119*, 4021) in which all the parameters were obtained with the density functional theory. The accuracy together with the requirements of the computation was discussed in terms of positions of the charge response sites and choice of a basis set. The calculated permittivities of typical organic compounds turned out to agree with the experimentally obtained values in the deviation of about 7% when a reasonable computational cost was maintained.

Introduction

Static permittivities of organic molecular crystals are currently important parameters with relation to their electrical and optical properties in the field of organic electronics. The static permittivity tensor of a crystal is indispensable to discuss, for example, the charge carrier mobility in the crystal[1] and the second harmonic generation (SHG) in a nonlinear optical material.[2] However, only a limited amount of experimental data is available for static permittivities of organic crystals, since it is in general difficult to obtain large organic crystals with high anisotropy. A reliable calculation method to evaluate static permittivities will therefore be useful for organic crystals.

The static permittivity of a dielectric material includes three kinds of polarizations: orientation polarization, atomic polarization, and electronic polarization.[3] In organic crystals the orientation polarization is not significant as the molecular dipoles are rigidly fixed to the lattice.[4] On the other hand, the contributions of the electronic and atomic polarizations are efficiently large, while the atomic one is evidently small in the case of rigid molecules.[5,6] As most molecules applied to organic electronic devices are π-conjugated and rigid, only the electronic polarization should be taken into account for the calculation of the static permittivity.

Several different methods for calculating the static permittivity tensor in terms of the electronic polarization have so far been reported. In the rigorous local field (RLF) theory proposed by Munn and Hurst[7−9] a molecular polarizability is obtained from a quantum chemical calculation and is empirically divided into a set of site polarizabilities, which means that a molecule is regarded as a set of polarizable sites.[10,11] Then the static permittivity tensor is calculated from the site polarizabilities under a local electric field in the crystal. The local electric field at a molecule in the crystal is rigorously calculated as a sum of external electric field and internal electric field induced from the other molecules in the crystal. It is noted that the resulting permittivity depends effectually on how to divide the molecular polarizability.

Morita and Kato proposed the charge response kernel theory in the simulation of molecular dynamics in liquid solution.[12−15] In this theory molecular polarization is regarded as charge redistribution in a molecule, explicitly computed using the charge response kernel (CRK) as $(\partial q/\partial V)$, where Δq is intramolecular charge redistribution under the applied electric potential V. CRK obtained from the quantum chemical calculation enables us to compute the molecular polarization without the empirical treatment. Soos et al. applied the CRK theory to calculate static permittivity tensors of organic crystals[16] using the semiempirical INDO/S Hamiltonian[17] to obtain CRK, i.e., the semiempirical charge response kernel (S-CRK). The molecular polarization is divided into nonlocal and atomic components. The nonlocal component stands for redistribution of delocalized charges and is computed using the S-CRK. On the other hand, the atomic component represents induced atomic dipoles normal to the molecular plane which are computed from atomic polarizabilities allocated empirically on all the atoms in a molecule. This means the resulting permittivity tensor depends on the way of allocation.

In this paper we will apply an imaginary site for the calculation of CRK where both the nonlocal and the atomic components of molecular polarization are explicitly evaluated without empirical treatment. Further, we use the density functional theory to calculate CRK (DFT-CRK) in place of INDO/S theory.[18] These differences are expected to result in more accurate permittivity tensors for various kinds of organic compounds in comparison with those on the basis of S-CRK.

For the estimation of accuracy and computational cost of DFT-CRK, we calculated static permittivity tensors of different kinds of organic compounds, e.g., polycyclic aromatic hydrocarbons, nonlinear optical materials, and organic semiconductors, enabling us to compare the obtained results with the available experimental data.

---

* Corresponding authors: Jun'ya Tsutsumi, tel +81-29-861-2582, fax +81-29-861-2586, e-mail junya.tsutsumi@aist.go.jp; Naoki Sato, tel +81-774-38-3080, fax +81-774-38-3084, e-mail naokis@e.kuicr.kyoto-u.ac.jp.

† Institute for Chemical Research.

‡ Present address: Photonics Research Institute, National Institute of Advanced Industrial Science and Technology (AIST), Tsukuba 305-8562, Japan.

§ Pioneering Research Unit for Next Generation.

‖ Department of Chemistry, Graduate School of Science.

10.1021/jp903420w CCC: $40.75

Calculation

Static Permittivity. A static permittivity tensor is calculated on the basis of DFT-CRK as follows. The static permittivity tensor $\varepsilon_{\alpha\beta}$ of a crystal is expressed using a molecular dipole moment $\Delta\mu$ induced by external electric field E^{ext}[19]

$$\varepsilon_{\alpha\beta} = \delta_{\alpha\beta} + \frac{4\pi \sum_{i}^{\text{mol}} \Delta\mu_{\beta i}}{v E_{\alpha}^{\text{ext}}} \tag{1}$$

where δ and v are the Kronecker's delta and the unit cell volume, respectively. Subscripts α and β indicate arbitrary Cartesian components. $\Delta\mu$ is summed over all the molecules i in the unit cell. The induced molecular dipole moment $\Delta\mu$ on a molecule i is expressed as

$$\Delta\mu_{\alpha i} = \sum_{a}^{\text{atom}} (q_{ia}' - q_{ia}^{0}) r_{\alpha ia} \tag{2}$$

where r is a position of a charge response site (placed on the center of the atom in usual case) and q' and q^0 are partial atomic charges with and without an external electric field, respectively. r, q', and q^0 are summed over all the atoms a in molecule i. q' and q^0 are calculated[12] as

$$q_{ia} = q_{ia}^{\text{iso}} + \sum_{b}^{\text{atom}} K_{iab}(V_{ib} + E_{\alpha}^{\text{ext}} r_{\alpha ib}) \tag{3}$$

where q^{iso} is a partial atomic charge in an isolated molecule, and the second term corresponds to its change due to a local electrostatic potential ($V + E^{\text{ext}}r$) in the crystal. V corresponds to a potential given by surrounding molecules in the crystal, while $E^{\text{ext}}r$ is the potential due to the external electric field E^{ext}. V is expressed as

$$V_{ia} = \sum_{j\neq i}^{\text{mol}} \sum_{b}^{\text{atom}} \frac{q_{jb}}{|\mathbf{r}_{jb} - \mathbf{r}_{ia}|} \tag{4}$$

using partial atomic charges q in the surrounding molecules. The eqs 3 and 4 are solved so that q and V become self-consistent with each other. q' and q^0 are a self-consistent solution of the eq 3 with and without the external electric field E^{ext}, respectively. In the calculation of V, we employed the Ewald summation method[20] to correct the long-range electrostatic interactions, making the expression of the eq 4 slightly more complicated. K in eq 3 is CRK defined[12] as

$$K_{iab} = \frac{\partial q_{ia}}{\partial V_{ib}} \tag{5}$$

which is a matrix for atoms a and b and expresses a response of a partial atomic charge q on the atom a with respect to an electrostatic potential V on the atom b in a molecule i. K can denotes nonlocal charge redistribution through the off-diagonal elements. Such nonlocal polarization should be crucial to π-conjugated molecules.[12] K satisfies equation[12]

$$\sum_{a}^{\text{atom}} K_{iab} = \sum_{b}^{\text{atom}} K_{iab} = 0 \tag{6}$$

This relation corresponds to charge neutralization of a molecule during the charge redistribution process. K is related to a molecular polarizability tensor $\alpha_{\alpha\beta i}$ with the following equation[13]

$$\alpha_{\alpha\beta i} = -\sum_{a,b}^{\text{atom}} K_{iab} r_{\alpha ia} r_{\beta ib} \tag{7}$$

q^{iso} and K were calculated using a package software GAMESS,[21] source code of which was modified for DFT-CRK calculation. The Breneman fitting method[22] was applied to obtain q^{iso} and K under the electrostatic potential of a molecule owing to quantum mechanical calculation. The molecular orbital calculation was carried out at the B3LYP level with several kinds of different basis sets. With the obtained q^{iso} and K, $\varepsilon_{\alpha\beta}$ was calculated by a Fortran77 code prepared by ourselves.

Imaginary Sites. In the CRK theory charge response sites are allocated on all the atomic positions in a molecule.[12] Since electronic polarization comes to be represented as charge redistribution among charge response sites, at least two response sites are necessary to express the polarization. However, a planar molecule has only one response site in the direction perpendicular to the molecular plane, disabling to express the electronic polarization in this direction.[14] We therefore add imaginary charge response sites above and below the molecular plane. Figure 1a shows the naive model with no imaginary (NI) site and two kinds of imaginary site models: Figure 1b ring-centered (RC) sites and Figure 1c ring-membered atomic (RMA) sites. In the RC model the imaginary sites are positioned at a distance d above and below the center of a six-membered ring, while they are positioned at d above and below all the ring-membered atoms in the RMA model. We applied these three models to calculate permittivities of organic crystals to compare the respective results with each other.

Crystal Structure. Calculation of a static permittivity tensor was carried for 15 kinds of organic compounds including polycyclic aromatic hydrocarbons, perylene-3,4,9,10-tetracarboxylic dianhydride (PTCDA), 3-methyl-4-nitropyridine *N*-oxide (POM),[23] and 4-methoxy-3-methyl-4′-nitrostilbene (MMONS);[24] the latter two are known as nonlinear optical materials. Structural data of those crystals were taken from the reported results and used without further optimization; Tables 1, 2, and 3 contain a reference number for the structural data of each compound.

Computing Hardware. All calculations were carried out on a SGI Altix4700 supercomputer in parallel execution of 16 processors. CPU times shown below are total processing times for all the 16 processors.

Results and Discussion

Imaginary Site Dependence. Static permittivity tensors of benzene and naphthalene were calculated using the three models with different situations of imaginary sites to examine dependence on the choice of imaginary sites. Table 1 shows the static permittivity tensors calculated for the NI, RC, and RMA models with $d = 0.1$ nm for the latter two ones. Z3POL basis set[25] was employed to obtain these values. The observed permittivity tensors are also shown for comparison. In the case of the NI model the calculated tensor is in poor agreement with the observed one, most obviously for the tensor component along the molecular stacking direction in the crystal; the deviations

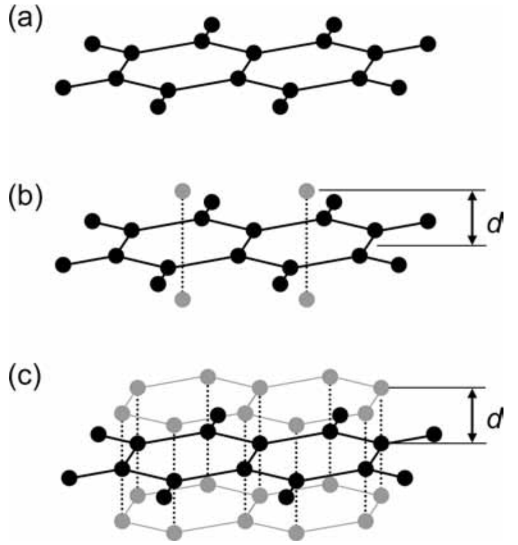

Figure 1. Schematic of charge response sites applied to calculation for naphthalene. The black and gray circles indicate charge response sites and imaginary charge response sites, respectively. (a) The charge response sites are allocated on each atom with no imaginary (NI) site. (b) Ring-centered (RC) imaginary sites are added at a distance *d* above and below the center of each six-membered ring. (c) Imaginary sites are added at ring-membered atomic (RMA) sites at *d* above and below each carbon atom.

are 25% and 30% for ε_{aa} and $\varepsilon_{c^*c^*}$, respectively, in the case of benzene, and that is 36% for ε_{aa} in the case of naphthalene. These deviations rely on molecular polarizability tensors calculated with eq 7. The molecular polarizability tensor is also shown in Table 1 together with that calculated on the basis of the finite field (FF) perturbation theory for comparison.[26] The finite field polarizability can be taken as a reference value of calculation with the highest accuracy. The out-of-plane component of polarizability, α_{33}, in the NI model in all the cases completely fails to approach that in the finite field one. This leads to the incorrect result of the static permittivity for the tensor component in the molecular stacking direction. On the other hand, α_{33} calculated for the RC and RMA models approaches the finite field value, and the static permittivity tensors calculated for the RC and RMA models deviate only 5% and 9% from the observed values for benzene and naphthalene, respectively. These results show that the imaginary sites work efficiently to express the out-of-plane polarization in the case of benzene and naphthalene. It is noted that the static permittivity tensors calculated for the RC and RMA models are very similar; the difference is less than 3%. Since computational cost was lower in the RC model, we applied the RC model in the following calculations.

Dependence of the components of a static permittivity tensor on the distance of imaginary sites from the molecular plane, *d*, in the RC model is shown for naphthalene in Figure 2. As seen in the figure the permittivity is calculated to be independent of *d* above 0.02 nm. We therefore set $d = 0.10$ nm for further calculations.

Basis Set Dependence. Static permittivity tensors of benzene and naphthalene were calculated using different kinds of basis sets as follows, aug-cc-pVTZ,[31] POL,[32] Z3POL,[25] and 6-31+G(d).[33] The obtained results are shown in Table 2. Aug-cc-pVTZ is a valence triple-ζ basis set being useful for accurate calculations of molecular polarizability and electric multipoles. It is very demanding computationally, which makes difficult to apply it to large organic molecules. In Table 2 the obtained values are regarded as the reference values of calculation in the highest accuracy. 6-31+G(d) is a low cost basis set whose CPU time is about one fiftieth of that of aug-cc-pVTZ. However, the accuracy is insufficient as the calculated tensor components are about 6% smaller than those of aug-cc-pVTZ. POL and Z3POL are polarized basis sets particularly developed for calculating dielectric properties.[25,32] They give good results for relatively small computational costs; their calculated values coincide with those of aug-cc-pVTZ to within 1%. Since the computational cost of Z3POL is lower than that of POL, we conclude that Z3POL provides us with the best compromise for computational cost and accuracy among the basis sets tested above.

Comparison with Experimental and Differently Calculated Results. Using the optimized imaginary site condition and the basis set for the CRK calculation mentioned above, we calculated static permittivity tensors of 15 kinds of organic compounds. The calculated permittivity tensors shown in Table 3 agree with the observed ones to within 7% for benzene, naphthalene, PTCDA, POM, and MMONS. In the case of anthracene the tensor component, ε_{11}, is smaller than the observed one by 13%, whereas the differences of ε_{22} and ε_{33} from the observed values fall within 6%. This might be due to an experimental error of the observed ε_{11} value which is scattered in the range of 2.3−2.6 for the different reports.[34−37] In Table 4 we compare the averaged permittivities for phenanthrene, chrysene, pyrene, perylene, biphenyl, *p*-terphenyl, *p*-benzoquinone, durene, and 1,4-dioxane, since only scalar values

TABLE 1: Static Permittivity Tensors with Molecular Polarizability Tensors Calculated Using the NI, RC and RMA Models in Comparison with Experimental Values for Benzene and Naphthalene[a]

compound	crystal data	model	ε			$\alpha/10^{-41}$ F m^2			CPU time/s
			aa	*bb*	*c*c**	11	22	33	
benzene	27	NI	1.78	2.52	1.67	129.60	128.22	0.10	9194
		RC	2.44	2.57	2.37	128.87	127.90	64.37	10918
		RMA	2.40	2.62	2.38	125.60	126.95	71.01	17844
		FF				134.24	132.78	71.31	
		exp.[28]	2.38	2.71	2.40				
naphthalene	29	NI	1.69	2.44	3.47	268.42	198.20	0.02	51931
		RC	2.46	2.98	3.22	268.16	197.63	89.86	60292
		RMA	2.39	2.88	3.15	264.26	196.44	97.73	103365
		FF				276.54	206.06	105.36	
		exp.[30]	2.65	2.87	3.21				

[a] Crystal data employed for the calculations are cited from the references. Molecular polarizability tensors calculated using the FF method are also shown for comparison. *a* and *b* indicate crystal axes of the unit cell, and *c** denotes a crystal axis normal to both *a* and *b* axes. 1, 2, 3 mean principal axes of the molecular polarizability tensor. Total CPU time is shown for a measure of computational cost.

TABLE 2: Static Permittivity Tensors Calculated with Different Basis Sets[a]

compound	crystal data	basis set	ε_{aa}	ε_{bb}	$\varepsilon_{c^*c^*}$	$\bar{\varepsilon}$	CPU time/s
benzene	27	aug-cc-pVTZ	2.46	2.58	2.39	2.48	165864
		POL	2.44	2.57	2.37	2.46	17375
		Z3POL	2.44	2.57	2.37	2.46	10918
		6-31+G(d)	2.29	2.45	2.24	2.32	3759
naphthalene	29	aug-cc-pVTZ	2.49	3.00	3.23	2.91	1296630
		POL	2.47	2.99	3.23	2.90	127957
		Z3POL	2.46	2.98	3.22	2.89	60292
		6-31+G(d)	2.35	2.81	3.08	2.75	21811

[a] Crystal data employed for the calculations are cited from the references. *a* and *b* indicate crystal axes of the unit cell, and *c** denotes a crystal axis normal to both *a* and *b* axes. $\bar{\varepsilon}$ stands for the average permittivity. CPU time is shown for a measure of computational cost.

TABLE 3: Static Permittivity Tensors Calculated Using DFT-CRK for Six Kinds of Organic Crystals[a]

compound	crystal data	method	ε_{xx}	ε_{yy}	ε_{zz}	$\bar{\varepsilon}$	axis
benzene	27	DFT-CRK	2.44	2.57	2.37	2.46	$x = a, y = b, z = c^*$
		RLF1[38]	2.39	2.67	2.41	2.49	
		RLF6[38]	2.35	2.69	2.35	2.46	
		exp.[28]	2.38	2.71	2.40	2.50	
naphthalene	29	DFT-CRK	2.46	2.98	3.22	2.89	$x = a, y = b, z = c^*$
		RLF1[10]	3.17	3.79	2.65	3.20	
		RLF2[10]	2.64	3.39	2.99	3.01	
		RLF10[10]	2.55	3.01	3.31	2.96	
		exp.[30]	2.65	2.87	3.21	2.91	
anthracene	39	DFT-CRK	2.18	2.81	3.88	2.96	$x = 1, y = 2, z = 3$
		S-CRK[16]	2.23	2.91	4.03	3.06	
		exp.[35]	2.51	2.99	4.11	3.20	
PTCDA	40	DFT-CRK	1.92	4.00	4.03	3.32	$x = 1, y = 2, z = 3$
		S-CRK[16]	1.96	3.98	4.00	3.22	
		exp.[41]	1.85	4.07	4.07	3.33	
POM	42	DFT-CRK	2.56	3.24	2.52	2.77	$x = a, y = b, z = c^*$
		exp.[43]	2.76	3.33	2.58	2.89	
MMONS	44	DFT-CRK	2.23	2.64	3.56	2.81	$x = a, y = b, z = c^*$
		exp.[45]	2.33	2.63	3.76	2.91	

[a] The values calculated using RLF and S-CRK together with the experimental ones are also shown for comparison. Crystal data employed for the calculations are cited from the references. *a* and *b* indicate crystal axes of the unit cell, and *c** denotes a crystal axis normal to both *a* and *b* axes. 1, 2, 3 mean principal axes of the static permittivity tensor. Key: PTCDA, perylene-3,4,9,10-tetracarboxylic dianhydride; POM, 3-methyl-4-nitropyridine *N*-oxide; MMONS, 4-methoxy-3-methyl-4′-nitrostilbene.

TABLE 4: Static Permittivity Tensors Calculated Using DFT-CRK in Comparison with Experimental Average Values, $\bar{\varepsilon}_{\text{exp}}$, for Nine Kinds of Organic Crystals[a]

compound	crystal data	ε_{xx}	ε_{yy}	ε_{zz}	$\bar{\varepsilon}$	$\bar{\varepsilon}_{\text{exp}}$	axis
phenanthrene	46	2.30	2.70	3.24	2.75	2.96[47]	$x = a, y = b, z = c^*$
chrysene	48	2.54	2.95	3.57	3.02	3.09[47]	$x = a, y = b, z = c^*$
pyrene	49	3.00	2.58	3.68	3.09	3.19[50]	$x = a, y = b, z = c^*$
perylene	51	3.50	3.04	2.60	3.05	3.34[47]	$x = a, y = b, z = c^*$
biphenyl	52	2.47	2.54	3.11	2.71	2.88[47]	$x = a, y = b, z = c^*$
p-terphenyl	53	2.63	2.70	3.80	3.05	2.98[47]	$x = a, y = b, z = c^*$
p-benzoquinone	54	2.17	2.91	1.92	2.33	2.66[55]	$x = a, y = b, z = c^*$
durene	56	2.18	2.22	2.32	2.24	2.55[47]	$x = a, y = b, z = c^*$
1,4-dioxane	57	2.04	2.07	2.00	2.04	2.28[55]	$x = a, y = b, z = c^*$

[a] Crystal data employed for the calculations are cited from the references. *a* and *b* indicate crystal axes of the unit cell, and *c** denotes a crystal axis normal to both *a* and *b* axes.

of observed permittivities are reported for these compounds. The calculated average values agree with the observed ones within the difference by 7% for all these compounds. Thus our DFT-CRK method turned out to provide us with notable accuracy and versatility for the calculation of permittivity tensors of organic crystals. The calculation on relatively large molecules in Table 3 was time-consuming to a degree, e.g., the CPU time for PTCDA was 2800000 s. For such large molecules low-cost basis sets are eligible while the accuracy of the obtained result could be lowered to some extent.

In Table 3 we compare static permittivity tensors calculated using DFT-CRK with those calculated using other methods: RLF[10,38] and S-CRK.[16] In the case of RLF two and three sets of permittivity tensors have been calculated with different numbers of polarizable sites standing for a molecule of benzene and naphthalene, respectively. For instance, a benzene molecule is regarded as a single polarizable point in RLF1 and as six polarizable points in RLF6.[10,38] The static permittivity tensors calculated using DFT-CRK for benzene and naphthalene agree with those calculated using RLF6 and RLF10 to within 5% and 4%, respectively. However, in the case of naphthalene large disagreements are noted between the values calculated using RLF1 and RLF2; the respective differences are 29% and 14%. This indicates that the static permittivity tensor calculated using RLF depends strongly on the selection of local sites describing a molecular polarizability. Such a problem is also noted in the

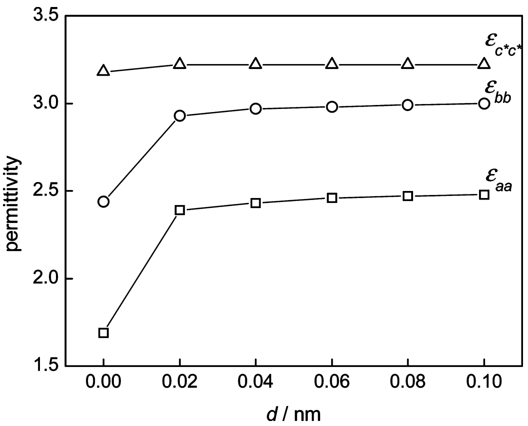

Figure 2. Permittivity tensor components calculated using the RC model for naphthalene versus a distance d between the imaginary sites and the molecular plane. a and b indicate crystal axes of the unit cell, and c^* denotes a crystal axis normal to both a and b axes.

case of the DFT-CRK results where imaginary sites must be introduced to express an out-of-plane component of a molecular polarizability. However, it should be recognized that CRK on all the sites are uniquely calculated using the Breneman fitting method[22] where CRK is calculated so as to reproduce electrostatic potentials at the grid points located on the molecular surface. On the other hand, site polarizabilities in the RLF method are arbitrarily allocated with no definite procedure unlike the Breneman fitting method. Thus, CRK represents electrostatic response of a molecule more reasonably than the arbitrarily allocated site polarizability, which is definitely crucial to obtain an accurate permittivity tensor. This advantage will particularly be notable in the case of low-symmetry molecules where arbitrarily allocated site polarizability is fairly questionable.

Permittivity tensors of anthracene and PTCDA calculated using DFT-CRK agree with those calculated using S-CRK[16] to within 4% and 2%, respectively. Thus, DFT-CRK and S-CRK give the values with comparative accuracies for these relatively simple molecules. However, the INDO/S Hamiltonian has been reported to give sometimes incorrect results due to its semiempirical nature;[18,58,59] S-CRK could provide us with wrong permittivities for exotic materials. On the other hand, DFT-CRK is expected to give accurate results for various kinds of compounds as it is based on the first principle density functional theory. We should, however, be aware that the density functional theory on the basis of conventional exchange functionals fails bitterly the evaluation of field-induced properties in the case of π-conjugated-chain molecules such as polyacetylene.[60] We must therefore employ the DFT-CRK method with great care in such particular cases. In this concern some trials to improve the DFT fault have been reported.[61,62] These trials will enable us to obtain correct permittivity tensors using DFT-CRK even in the case of π-conjugated-chain molecules.

Conclusion

The static permittivity tensors of organic molecular crystals were calculated by the charge response kernel theory in which all the parameters were obtained with the density functional theory. Use of the first principle DFT gives accurate and reliable values for all the crystals tested in this work. In order to account for the electronic-polarization component normal to the molecular plane, imaginary sites were added. It was found that the ring-centered (RC) imaginary site with the basis set of Z3POL provides us with the best compromise for computational cost and accuracy.

Acknowledgment. Computation was carried out at the SuperComputer Laboratory, Institute for Chemical Research, Kyoto University. The authors are grateful to Mr. Fumihito Mohri at Kaneka Co. for the information of observed permittivity tensors of organic crystals. This work was partially supported by a MEXT Joint Project of Chemical Synthesis Core Research Institutions from the Ministry of Education, Culture, Sports, Science and Technology of Japan.

References and Notes

(1) Munn, R. W. *Chem. Phys. Lett.* **1972**, *16*, 429.

(2) Chemla, D. S.; Zyss, J. *Nonlinear Optical Properties of Organic Molecules and Crystals*; Academic Press: 1987; Vol. 1.

(3) Kittel, C. *Introduction to Solid State Physics*; 7th ed.; John Wiley and Sons: New York, 1996.

(4) Fröhlich, H. *Theory of Dielectrics; Dielectric Constant and Dielectric Loss*, 2nd ed.; Clarendon Press: Oxford, 1958.

(5) Le Fèvre, R. J. W.; Narayana Rao, D. A. A. S. *Aust. J. Chem.* **1955**, *8*, 39.

(6) Coop, I. E.; Sutton, L. E. *J. Chem. Soc.* **1938**, 1269.

(7) Munn, R. W. *Chem. Phys.* **1980**, *50*, 119.

(8) Hurst, M.; Munn, R. W. *J. Mol. Electron.* **1986**, *2*, 35.

(9) Hurst, M.; Munn, R. W. *J. Mol. Electron.* **1986**, *2*, 43.

(10) Reis, H.; Papadopoulos, M. G.; Calaminici, P.; Jug, K.; Köster, A. M. *Chem. Phys.* **2000**, *261*, 359.

(11) Le Sueur, C. R.; Stone, A. J. *Mol. Phys.* **1994**, *83*, 293.

(12) Morita, A.; Kato, S. *J. Am. Chem. Soc.* **1997**, *119*, 4021.

(13) Morita, A.; Kato, S. *J. Chem. Phys.* **1998**, *108*, 6809.

(14) Iuchi, S.; Morita, A.; Kato, S. *J. Phys. Chem. B* **2002**, *106*, 3466.

(15) Ishida, T.; Morita, A. *J. Chem. Phys.* **2006**, *125*, 074112.

(16) Soos, Z. G.; Tsiper, E. V.; Pascal, R. A., Jr. *Chem. Phys. Lett.* **2001**, *342*, 652.

(17) Zerner, M. C.; Loew, G. H.; Kirchner, R. F.; Mueller-Westerhoff, U. T. *J. Am. Chem. Soc.* **1980**, *102*, 589.

(18) Isborn, C. M.; Leclercq, A.; Vila, F. D.; Dalton, L. R.; Brédas, J. L.; Eichinger, B. E.; Robinson, B. H. *J. Phys. Chem. A* **2007**, *111*, 1319.

(19) Oka, S. *Yudentairon (Theory of Dielectrics)*; Gendai Kogakusha: Tokyo, 1954.

(20) Frenkel, D.; Smit, B. *Understanding Molecular Simulation*, 2nd ed.; Academic Press, 2002.

(21) Schmidt, M. W.; Baldridge, K. K.; Boatz, J. A.; Elbert, S. T.; Gordon, M. S.; Jensen, J. H.; Koseki, S.; Matsunaga, N.; Nguyen, K. A.; Su, S. J.; Windus, T. L.; Dupuis, M.; Montgomery, J. A. *J. Comput. Chem.* **1993**, *14*, 1347.

(22) Breneman, C. M.; Wiberg, K. B. *J. Comput. Chem.* **1990**, *11*, 361.

(23) Zyss, J.; Chemla, D. S.; Nicoud, J. F. *J. Chem. Phys.* **1981**, *74*, 4800.

(24) Tam, W.; Guerin, B.; Calabrese, J.; Stevenson, S. *Chem. Phys. Lett.* **1989**, *154*, 93.

(25) Benkova, Z.; Sadlej, A. J.; Oakes, R. E.; Bell, S. E. J. *J. Comput. Chem.* **2005**, *26*, 145.

(26) Kurtz, H. A.; Stewart, J. J. P.; Dieter, K. M. *J. Comput. Chem.* **1990**, *11*, 82.

(27) Bacon, G.; Curry, N.; Wilson, S. *Proc. R. Soc. London, Ser. A* **1964**, *279*, 98.

(28) Hochstrasser, R. M.; Meredith, G. R.; Trommsdorff, H. P. *J. Chem. Phys.* **1980**, *73*, 1009.

(29) Alt, H.; Kalus, J. *Acta Crystallogr., Sect. B* **1982**, *38*, 2595.

(30) Munn, R. W.; Williams, D. F. *J. Chem. Phys.* **1973**, *59*, 1742.

(31) Dunning, T. H., Jr. *J. Chem. Phys.* **1989**, *90*, 1007.

(32) Sadlej, A. J. *Chem. Phys. Lett.* **1977**, *47*, 50.

(33) Hehre, W. J.; Ditchfield, R.; Pople, J. A. *J. Chem. Phys.* **1972**, *56*, 2257.

(34) Dix, G.; Helberg, H. W.; Wartenberg, B. *Phys. Status Solidi A* **1971**, *5*, 633.

(35) Karl, N.; Rohrbacher, H.; Siebert, D. *Phys. Status Solidi A* **1971**, *4*, 105.

(36) Nakada, I. *J. Phys. Soc. Jpn.* **1962**, *17*, 113.

(37) Munn, R. W.; Nicholson, J. R.; Schwob, H. P.; Williams, D. F. *J. Chem. Phys.* **1972**, *58*, 3828.

(38) Reis, H.; Raptis, S.; Papadopoulos, M. G.; Janssen, R. H. C.; Theodorou, D. N.; Munn, R. W. *Theor. Chem. Acc.* **1998**, *99*, 384.

(39) Brock, C.; Dunitz, J. *Acta Crystallogr., Sect. B* **1990**, *46*, 795.

(40) Tojo, K.; Mizuguchi, J. *Z. Kristallogr.* **2002**, *217*, 253.

(41) Zang, D. Y.; So, F. F.; Forrest, S. R. *Appl. Phys. Lett.* **1991**, *59*, 823.

(42) Baert, F.; Schweiss, P.; Heger, G.; More, M. *J. Mol. Struct.* **1988**, *178*, 29.

(43) Dou, S. X.; Josse, D.; Zyss, J. *J. Opt. Soc. Am. B* **1991**, *8*, 1732.

(44) Suh, I.; Lim, S.; Lee, J.; Ryu, B.; Kim, M.; Yoon, C. S.; Hong, H.; Lee, K. S. *Acta Crystallogr., Sect. C* **1994**, *50*, 1768.

(45) Bierlein, J. D.; Cheng, L. K.; Wang, Y.; Tam, W. *Appl. Phys. Lett.* **1990**, *56*, 423.

(46) Petricek, V.; Cisarova, I.; Hummel, L.; Kroupa, J.; Brezina, B. *Acta Crsytallogr., Sect. B* **1990**, *46*, 830.

(47) Ishii, K.; Kinoshita, M.; Kuroda, H. *Bull. Chem. Soc. Jpn.* **1973**, *46*, 3385.

(48) Burns, D. M.; Iball, J. *Proc. R. Soc. London, Ser. A* **1960**, *257*, 491.

(49) Camerman, A.; Trotter, J. *Acta Crystallogr.* **1965**, *18*, 636.

(50) Price, A. H.; Williams, J. O.; Munn, R. W. *Chem. Phys.* **1976**, *14*, 413.

(51) Nather, C.; Bock, H.; Havlas, Z.; Hauck, T. *Organometallics* **1998**, *17*, 4707.

(52) Charbonneau, G.; Delugeard, Y. *Acta Crystallogr., Sect. B* **1977**, *33*, 1586.

(53) Rietveld, H. M.; Maslen, E. N.; Clews, C. J. B. *Acta Crystallogr., Sect. B* **1970**, *26*, 693.

(54) van Bolhuis, F.; Kiers, C. T. *Acta Cryst. B* **1978**, *34*, 1015.

(55) *Kagakubenran (Handbook of Chemistry) Basic Edition*, 3rd ed.; Iwasawa, Y., Ed.; Maruzen: Tokyo, 1984.

(56) Stam, C. H. *Acta Crystallogr., Sect. B* **1972**, *28*, 2630.

(57) Koritsanszky, T.; Strumpel, M.; Buschmann, J.; Luger, P.; Hansen, N.; Pichon-Pesme, V. *J. Am. Chem. Soc.* **1991**, *113*, 9148.

(58) Yang, W.; Schatz, G. C. *J. Chem. Phys.* **1992**, *97*, 3831.

(59) Abe, J.; Shirai, Y. *J. Am. Chem. Soc.* **1996**, *118*, 4705.

(60) Champagne, B.; Perpète, E. A.; van Gisbergen, S. J. A.; Baerends, E.; Snijders, J. G.; Soubra-Ghaoui, C.; Robins, K. A.; Kirtman, B. *J. Chem. Phys.* **1998**, *109*, 10489.

(61) Baer, R.; Neuhauser, D. *Phys. Rev. Lett.* **2005**, *94*, 043002.

(62) Sekino, H.; Maeda, Y.; Kamiya, M.; Hirao, K. *J. Chem. Phys.* **2007**, *126*, 014107.

JP903420W